[Geophyiscal Research Letters]

Supporting Information for

[Heterotrophy of oceanic particulate organic matter elevates net ecosystem calcification]

[Andrea K. Kealoha[1*], Kathryn E.F. Shamberger[1], Emma Reid[2], Kristen Davis[2], Steven Lentz[3], Russell E. Brainard[4], Thomas Oliver[4], Michael S. Rappé[5], Brendan Roark[1], Yoshimi M. Rii[5]]

[[1]Department of Oceanography, Texas A&M University, College Station, TX, 77843
[2]Department of Civil & Environmental Engineering, University of California, Irvine, CA, 92697
[3]Woods Hole Oceanographic Institution, Woods Hole, MA, 02543
[4]Pacific Islands Fisheries Science Center, National Oceanic and Atmospheric Administration, Honolulu, HI, 96818
[5]Hawai'i Institute of Marine Biology, School of Ocean and Earth Science and Technology, University of Hawai'i at Mānoa, Kāne'ohe, HI, 96744]

Contents of this file

Additional Supporting Information (Files uploaded separately)

Introduction

The supplemental information includes a detailed description of the methods and calculations used in this study. The flow paths for individual water parcels sampled at sites 2 and 3 are shown in Figure S1. Figure S2 shows the flow paths for water samples removed from the analysis. Figure S3 provides the TA-S mixing lines of offshore and lagoon water, and the TA-S signatures of the reef samples. Figure S4 shows correlations of flow speed to NEC and $POC_{oc\text{-}up}$. The supplementary tables provide the depths and geographic coordinates of sampling sites (Table S1), means±std dev of input parameters

to NEC, NEP and POC_{oc_up} (Table S2), average NEC, NEP and $POC_{oc\text{-}up}$ at each of the sites (Table S3), the statistical summary for all relevant Model 2 linear regressions (Table S4), major benthic categories along the transect (Table S5), average $\delta^{13}C$ and % contribution values for each of the components used in the estimation for the $\delta^{13}C$ of reef particulate organic carbon (Table S6), and the uncertainties associated with each of the paramters used in the calculations for NEC, NEP and $POC_{oc\text{-}up}$ (Table S7)

Text S1

S1. Methods

S1.1 Site description

Kāneʻohe Bay (21.45° N, 157.80° W) is located on the northeast side of Oʻahu, Hawaiʻi (**Fig 1**). The estuarine bay has a total surface area of approximately 41 km^2 and consists of numerous patch and fringing reefs and two channels located on the north and south of a barrier reef (Jokiel, 1991). There have been numerous studies conducted in Kāneʻohe Bay and it is well characeterized in terms of its biogeochemistry, ecology, hydrodynamics and carbon system dynamics (Drupp et al., 2011; Lowe et al., 2009; Page et al., 2019; Terlouw et al., 2019). The CRIMP-2 buoy located on the lagoon-ward edge of the barrier reef displays high pCO_2 variability, which is primarily driven by organic carbon cycling, long water residence time and a shallow depth (Page et al., 2019; Terlouw et al., 2019). Despite a history of anthropogenic influences (e.g., urbanization, dredging and sewage discharge) that led to a dramatic decline in coral cover between the 1930s and 1970s, Kāneʻohe Bay corals have since rebounded and show a high resistance to ocean acidification and warming (Jokiel, 1991; Jury & Toonen, 2019).

To estimate coral cover in our study site, we conducted a video transect in nine segments across the reef flat, starting as close to the reef crest as possible (21.467840°N, -157.793560°W, segment 1), passing through sites 2 and 3, and ending right before the sandbar (21.463600°N, -157.799320°W, segment 9). Still images were taken from each

of the segments and analyzed in Coral Point Count software with Excel extensions (CPCe) using 10 random points per quadrat. The substrate was assigned one of five categories: (1) living coral; (2) macroalgae; (3) dead coral with algae; (4) coralline algae; and (5) sand/rubble (Kohler & Gill, 2006; **Table S5**). Some segments (e.g., segment 9) had a greater number of useable still images and so the data were normalized by adding the total % substrate across all images in a segment, divided by the number of images in that segment. A total of 30 still images were used to compute % substrate across the transect. Live coral cover ranged 0-10%, which is similar to the estimate of 5-10% measured in 2015 (Bahr et al., 2017). The major coral species in the bay are *Porites compressa* and *Montipora capitata*.

S1.2 Environmental data

Temperature and conductivity at stations 2 and 3 were measured with Seabird SBE-37 MicroCATs deployed on the reef. Surface water salinity and temperature were measured with each offshore and lagoon water sample using a SonTek Castaway CTD. Wind speed and photosynthetically active radiation (PAR) were measured at a weather station located on Moku o Loʻe at the Hawaiʻi Institute of Marine Biology (HIMB) (pacioos.hawaii.edu/weather/obs-mokuoloe/) in southern Kāneʻohe Bay, and offshore wave heights were obtained from the Coastal Data Information Program (CDIP) Buoy 098 located 4 miles south-east of Mokapu Point, Oahu (21.415 °N, -157.678 °W) in 88 m of water (http://cdip.ucsd.edu).

Nortek Aquadopp Acoustic Doppler current Profilers (ADP) were placed at stations 2, 3, 4 and 5 and measured current velocity profiles at 4-min intervals (**Fig. 1**). Current measurements were interrupted at sites 3 (23 Jan) and 5 (22 Jan) and were

therefore estimated for the remainder of the deployment using current measurements at site 2. To reconstruct currents at sites 3 and 5, a linear relationship between transport (U=u*h where u is water velocity and h is depth) at site 2 and site 3 or 5 was made when measurements were available. This relationship was used, along with measurements at site 2, to reconstruct currents at sites 3 and 5. To test this method, currents were reconstructed for periods where current measurements were available, and the R^2 between the actual and reconstructed currents was 0.73 ($p << 0.01$) at site 3 and 0.75 ($p << 0.01$) at site 5. To assess this method of reconstructing the currents, residence times were recalculated using reconstructed currents during deployment 1, when currents were available at all sites, and compared to actual residence time estimates. When using reconstructed currents at site 3 and 5, the average error in residence times during deployment 1 was 14%.

S1.3 Water sampling and analysis procedures

To minimize time differences in water sample collection between sites, two boats were deployed for each sampling trip (morning, noon, evening); one for the lagoon and offshore samples and one for the reef samples (sites 2 and 3). The offshore and reef samples were collected within an hour or less of each other, although one set of samples (1/14/17, noon) was collected over two hours. Hence, we assume that the minimal time lag between offshore and reef samples does not generate an additional uncertainty in the NEC and $POC_{oc\text{-}up}$ calculations.

Seawater samples for TA and DIC analyses were collected using a 2.5 L Niskin bottle deployed at 1-m depth. Water was transferred into 250 mL borosilicate glass bottles, fixed with 100 µL saturated mercuric chloride and sealed with Apiezon grease

(Dickson et al., 2007). TA and DIC were analyzed on a Versatile Instrument for the Determination of Total inorganic carbon and titration Alkalinity (VINDTA) 3C, which uses an open cell potentiometric titration for TA and coulometric titration for DIC. Certified Reference Materials (CRMs) were provided by A. Dickson (Scripps Institute of Oceanography) and used to standardize TA and DIC measurements (Dickson et al., 2007). The mean precision of these measurements was ±2.6 μmol kg^{-1} for DIC and ±2.0 μmol kg^{-1} for TA. Salinity-normalized TA (nTA) and salinity-normalized DIC (nDIC) were calculated using the average salinity (35) over the study. The remaining parameters of the carbonate system (e.g., pH, carbon dioxide partial pressure (pCO_2), Ω_{ar}) were calculated using CO2SYS (Pierrot et al., 2006) and the constants of Mehrbach et al. (1973) refit by Dickson and Millero (1987). Nutrient samples were analyzed using standard World Ocean Circulation Experiment (WOCE) segmented flow methodologies on an Astoria Analyzer (Astoria-Pacific) (WHP, 1994).

Samples for [POC] and δ^{13}C-POC analyses were obtained by filtering approximately 4 liters of seawater through pre-combusted glass-fiber filters (GF/F, Whatman) within 2 hours of collection, and stored in a -80 °C freezer until shipment to the Stable Isotope Geosciences Facility (SIGF) at Texas A&M University. The filters were acidified with HCl to remove inorganic carbon, rinsed with DI water and folded into tin capsules which were combusted with pure O_2 at 1020°C to CO_2 and analyzed using a Carlo Erba NA 1500 Series 2 Elemental Analyzer attached to a ThermoFinnigan Conflo III and a ThermoFinnigan Delta Plus XP isotope ratio mass spectrometer (IRMS). Raw sample δ^{13}C measurements are converted to the VPDB isotopic scales through an intra-run, two-point calibration of ~1 mg of L-glutamic acid standards (USGS 40 δ^{13}C = -

26.39‰ VPDB, and USGS 41 $\delta^{13}C$ = 37.63‰ VPDB). Internal laboratory standards are utilized as internal checks of the accuracy and precision of the calibrations. Precision of $\delta^{13}C$ was ±0.2‰ and ±0.2% for mass C (mg). Blank filters were also analyzed to check background levels which were negligible to non-existent.

S1.4 Residence times

To determine the residence time of water on the Kāneʻohe Bay reef flat, we used a quasi-Lagrangian framework similar to that used in DeCarlo et al. (2017). This involved tracing the path of a water parcel on the reef using estimated water velocity and tidally-corrected bathymetric data. For each seawater sample taken at site 2 or 3, the residence time was estimated by back-tracking in time, using depth-averaged velocity (in two-dimensions) and water depth (d) at the four ADPs, and bathymetry data from LiDAR (accuracy = ±0.15 m, https://www.coris.noaa.gov) for the whole reef. Velocities at each point were calculated by linearly interpolating the transport between the four ADPs, and when the water parcel was outside the bounds of the four stations, nearest-neighbor extrapolation was used. The sea level variation (η) at each time and the bathymetry (b, water depth relative to mean sea level) at each location were used to calculate a water depth (h) at each parcel location ($h = \eta + b$). Water parcels were tracked across the reef flat until they reached deeper water (3 m depth), and were deemed seaward of the reef crest.

Since many of the parcels originated to the north of our sampling sites, more information was needed to determine the transport in that section of the reef. When parcels were outside of the bounds of the four current meters, unphysical results were seen due to the nearest-neighbor extrapolation method. Lowe et al. (2009a) took current

measurements north of the transect (point A2, **Fig 1**). These current measurements, and a model of flow, were compared to the data that were taken during this deployment. Measured mean flow and direction at site A2 were similar in magnitude and direction to flow at site 3 during this deployment. The average depth at A2 was 2 m, and the average depth at site 3 was 1.7 m. Currents at site 3 were approximately 33% slower during this deployment, and the principal axes of site 3 major and minor components were approximately 13% and 34% smaller than at site A2, respectively. The orientation of the principal axes at site A2 was 246°, and site 3 was 277° for this deployment (Lowe et al., 2009). For the parcel tracing, the current data from site 3 were assumed to be similar enough to site A2, and were applied at the location of site A2 to expand the area where current data and depth could be interpolated for the parcel tracing.

The largest source of error in residence time is most likely the methodological assumption that the measured currents were representative of currents at A2. We estimated this error by performing a sensitivity analysis where we artificially relocated A2 and recalculated the residence times. We recalculated residence times for cases where A2 was moved 200 meters to the north, south, east and west on the reef, and this yielded a residence time error of up to 20%. This would affect the biogeochemical rates by approximately 25%.

S1.5 Calculations

NEC was calculated using the alkalinity anomaly method (Chisholm & Gattuso, 1991) shown in the following equation:

$$NEC = \frac{\Delta nTA \rho h_{avg}}{2t} \quad (1)$$

where ΔnTA is the change in nTA (μmol kg^{-1}) between the reef crest (defined here as 3-m depth) and site 2 or 3. We assume that the carbonate chemistry and POM chemistry of the water at our offshore sites was representative of water approaching the reef crest from offshore. ρ is seawater density (kg m^{-3}), h_{avg} is the time-averaged depth (m) of the water parcel and t is the estimated time (h) it took a water parcel to travel from the reef crest to site 2 or site 3 (i.e., residence time).

NEP was calculated using changes in DIC and correcting for the influence of NEC and air-sea CO_2 flux (F_{CO2}, mmol C m^{-2} d^{-1}) according to the equations:

$$NEP = \frac{\Delta nDIC \rho h_{avg}}{t} - NEC - F_{CO2} \quad (2)$$

$$F_{CO2} = ks(pCO_{2sw} - pCO_{2air}) \quad (3)$$

where ΔnDIC is the nDIC (μmol kg^{-1}) change from the reef crest to site 2 or 3, k is the gas transfer velocity (Ho et al., 2006), s is the solubility of CO_2 as a function of temperature and salinity (Weiss, 1974), and pCO_{2sw} and pCO_{2air} are the pCO_2 of seawater and air, respectively. pCO_{2sw} was calculated using our discrete TA and DIC measurements and CO2SYS (Pierrot et al., 2006) and pCO_{2air} was obtained from the CRIMP2 mooring located approximately 0.7 km south of site 3 (https://www.pmel.noaa.gov/co2/story/CRIMP2) (**Fig 1**).

In order to calculate oceanic POC uptake across the reef transect, we had to distinguish between POC produced by the reef and POC supplied to the reef from offshore. First, a two end-member isotope mixing model was used to determine the

concentration of oceanic POC ([POC_{oc}]) in the total POC pool. This equation is expressed as:

$$[POC_{oc}] = \frac{\delta^{13}C_{2(3)} - \delta^{13}C_{rf}}{\delta^{13}C_{oc} - \delta^{13}C_{rf}} * [POC_{2(3)}] \quad (4)$$

where $\delta^{13}C_{2(3)}$ is the measured isotopic composition of POC at either site 2 or 3, $\delta^{13}C_{rf}$ is the estimated isotopic composition of reef-derived POC, $\delta^{13}C_{oc}$ is the measured isotopic composition of offshore POC and [$POC_{2(3)}$] is the measured concentration of total POC at site 2 or 3. The $\delta^{13}C_{rf}$ was estimated from the literature assuming the major components of reef POM are coral mucus (30%), coral zooxanthellae (30%), fish feces (30%) and macroalgae (10%) (**Table S6**). The contributions of each component are based on Wyatt et al. (2013), who found roughly comparable releases of each component at Ningaloo reef, Australia. Average $\delta^{13}C$ of coral mucus (-15.9‰, range = -16.9 – -15‰) and zooxanthellae (-14.7‰, range = -15 – -14.5‰) were obtained from a study conducted in Kāneʻohe Bay, using the major coral species in the bay, *Porites* and *Montipora* (Rodrigues & Grottoli, 2006). To our knowledge, there are no published data on the isotopic composition of fish feces and macroalgae in Kāneʻohe Bay. Therefore, we obtained isotopic values for these components from coral reef studies conducted in Ningaloo reef and the Caribbean Sea (de la Moriniere et al., 2003; Wyatt et al., 2013). These studies report a range of $\delta^{13}C$ for fish feces and macroalgae (e.g., turf algae, *Halimeda*) as -17 to -12‰ (mean=-16.5‰) and -18.5 to -15‰ (mean=-17.5‰), respectively (**Table S6**). The weighted average $\delta^{13}C_{rf}$ was -15.87‰. Once [POC_{oc}] was determined, oceanic POC uptake ($POC_{oc\text{-}up}$) was calculated by:

$$POC_{oc-up} = \frac{\Delta POCh_{avg}}{t} \quad (5)$$

where ΔPOC is the change in [POC_{oc}] between the reef crest and site 2 or 3.

To acquire offshore TA, DIC, δ^{13}C-POC and [POC], water samples were collected offshore, 3 times a day. The offshore stations were positioned relatively close to the reef crest to ensure that the source water traversing the reef was characterized. During deployment 1, upstream values for each reef sample were determined by taking the time the water parcel started at the reef crest and using the offshore sample collected closest to that time. The deployment 1 offshore nTA and nDIC ranges were 2205-2289 μmol kg^{-1} and 1963-1987 μmol kg^{-1}, respectively. For deployment 2, three offshore samples (23-Jan 16:45, 24-Jan 07:32 and 16:46) were flagged as outliers. These three samples lay below the offshore TA-salinity mixing line and their temperature and heavier δ^{13}C values suggest a mix of offshore and lagoon water. These measurements also corresponded to periods of strong and predominantly northwest flow offshore during ebb tide, which indicates that this water may have continued offshore rather than flowing across the reef flat. As such, these measurements were removed. However, since removing these measurements leaves large gaps in the time-series of initial source water concentrations, we used the average offshore nTA (2301±4.85 μmol kg^{-1}), nDIC (1993±6.7 μmol kg^{-1}), and δ^{13}C (-26.24±1.64) for the entire second deployment. Important to note is that many of the flow paths, particularly for deployment 2, originate near Kapapa Island. The shallow waters surrounding the small island may modify the chemistry of source waters. Average surface (<15 m) nTA and nDIC at Hawaii Ocean Time-series (HOT,

http://hahana.soest.hawaii.edu/hot/) Station ALOHA located approximately 100 km north of Oahu (representing oligotrophic oceanic waters of the North Pacific Subtropical Gyre) was 2304±5.03 μmol kg^{-1} and 1978±11.09 μmol kg^{-1} from 1998-2017. Hence, although source waters during deployment 2 appear to originate northwest of our offshore sampling sites and near Kapapa Island, nTA and nDIC (and nDIC during deployment 1) were similar to HOT, suggesting relatively stable source water chemistry during deployment 2. Offshore nTA during deployment 1 was lower than HOT, which is consistent with the findings Fagan & Mackenzie (2007), Shamberger et al. (2011) and Courtney et al. (2018), who also measured lower TA immediately offshore of the Kaneohe Bay barrier reef crest relative to Station ALOHA.

The uncertainties in NEC, NEP and $POC_{oc\text{-}up}$, were estimated using a Monte Carlo approach ($n=10^4$), which propagates the uncertainties (standard deviation or standard error) of each of the parameters through the calculations (**Table S7**). To incorporate an uncertainty associated with the estimation for average $\delta^{13}C_{rf}$, we calculated $POC_{oc\text{-}up}$ assuming reef POC was composed of 100% macroalgae (i.e. the lightest of the reef components, $\delta^{13}C_{rf}$ =-17.5‰), and 100% zooxanthellae (i.e. the heaviest of the reef components, $\delta^{13}C_{rf}$ =-14.7‰). This introduced an ~18% uncertainty into the calculation. Excluding values not statistically different from 0, the relative standard deviations (%RSD) for NEC and NEP were approximately 30% and 40% for deployment 1 and 2, respectively. For $POC_{oc\text{-}up}$ uptake, %RSD was approximately 40% and 50% for deployment 1 and 2, respectively. The uncertainties increased ~10% during the second deployment due to the averaging of offshore values. For NEC, NEP and $POC_{oc\text{-}up}$, sources that contributed greatest to the total uncertainty were residence time during the

first deployment and the averaging of offshore TA, DIC and δ^{13}C-POC during the second deployment. To test for equality in means across deployments, we used a two-sample t-test (ttest2.m in matlab). Model II linear regression statistics are summarized in **Table S**4 and were performed using the matlab script lsqfitma.m provided by ET Peltzer (MBARI, https://www.mbari.org/products/research-software/matlab-scripts-linear-regressions/).

Figures

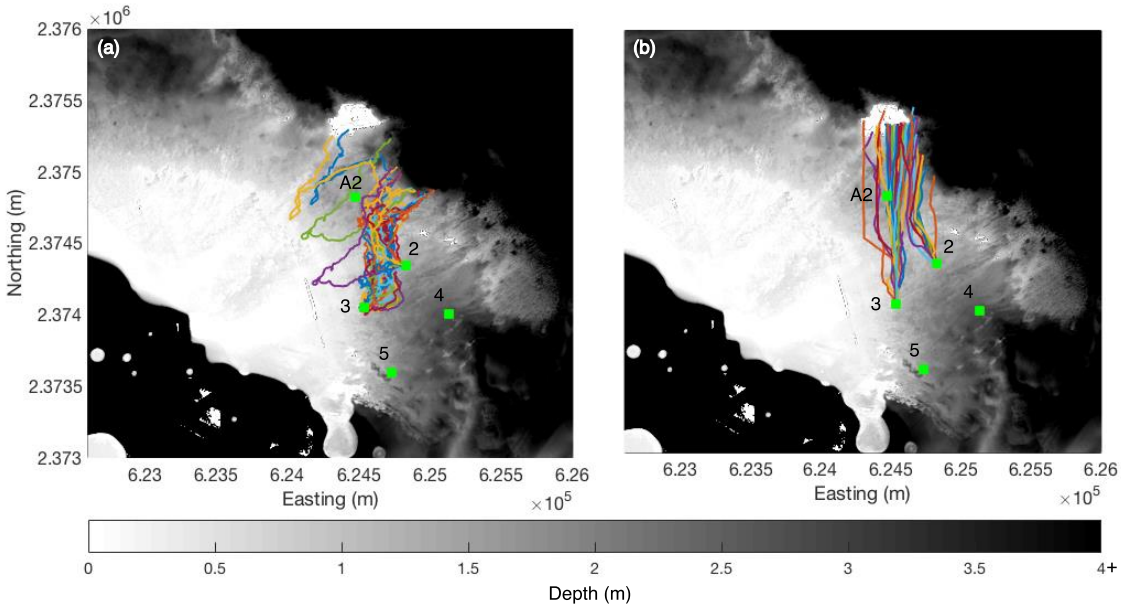

Figure S1: Flow paths for individual water parcels at sites 2 and 3 during (a) deployment 1 and (b) deployment 2. Both (a) and (b) include only the flow paths of samples used in NEC and $POC_{oc\text{-}up}$ calculations.

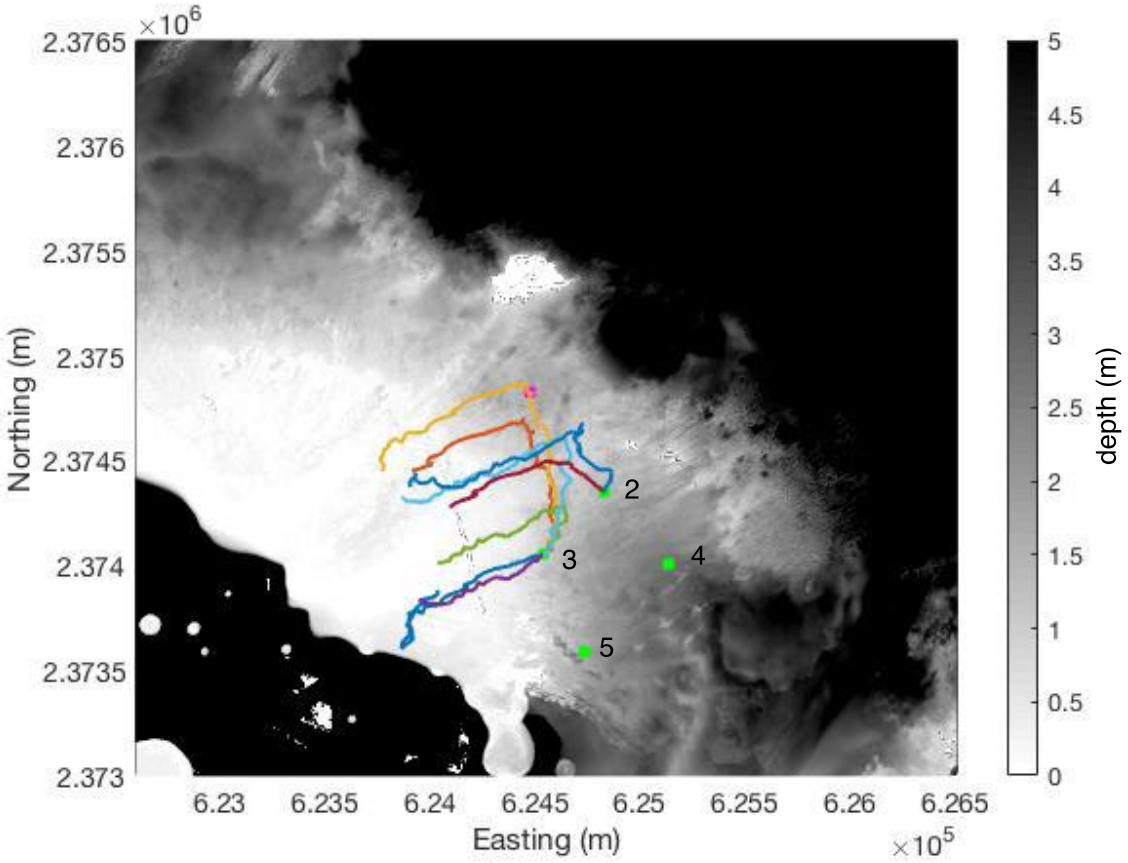

Figure S2: Flow paths for individual water parcels (i.e., samples) that were removed from the analysis because they traveled into the lagoon before being sampled on the reef or they were not traced back to the reef crest.

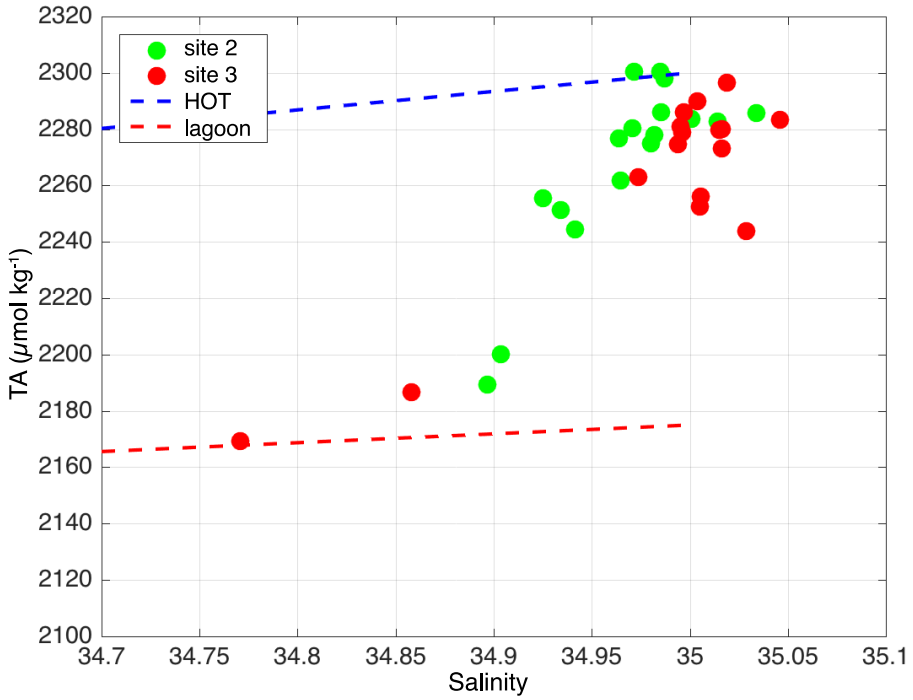

Figure S3: TA-salinity signatures of reef water samples at site 2 (green circles) and site 3 (red circles). The TA-salinity mixing line of the lagoon water (red dashed line) is based on data from this study, Courtney et al. (2018), Fagan and Mackenzie (2007) and Shamberger et al. (2011). The open ocean TA-S mixing line (blue dashed line) is determined from the surface water HOT data.

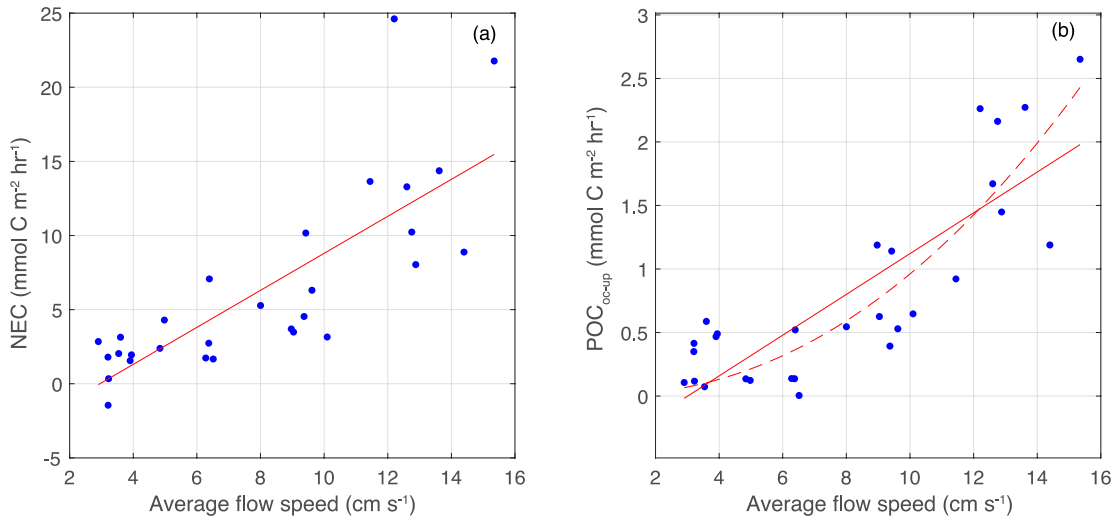

Figure S4: (a) Linear relationship (R^2=0.62) between average flow speed and NEC and (b) linear (R^2=0.69) and exponential (dashed line, R^2=0.76) relationships between average flow speed and $POC_{oc\text{-}up}$.

Tables

Site	Lat (°N)	Lon (°W)	Depth (m)
Offshore	21.47790	157.7858	10
2	21.46731	157.7952	1
3	21.46450	157.7981	1
4	21.46413	157.7923	3
5	21.46048	157.7962	2
Lagoon	21.45784	157.8053	13

Table S1: Geographic coordinates and depth of study sites.

	ΔnTA	$\Delta nDIC$	ρ	h_{avg}	t	F_{CO2}	ΔPOC
Deployment 1	21±18	7±42	1023.5±0.2	1.98±0.13	13.4±2.7	1.1±3.6	2.1±1.5
Deployment 2	20±9	18±48	1023.7±0.1	2.26±0.29	3.5±1.5	-2.5±6.0	1.2±0.7

Table S2: Means (±1 std dev) of ΔnTA (µmol kg^{-1}), ΔnDIC (µmol kg^{-1}), $\boldsymbol{\rho}$ (kg m^{-3}), h_{avg} (m), t (hrs), F_{CO2} (mmol C m^{-2} d^{-1}) and ΔPOC (mmol C m^{-3})

	Site 2 avg	Site 3 avg	Total avg	Total range
NEC				
Deployment 1	1.83±0.96	1.36±1.97	1.62±1.40	-1.45 to 3.14
Deployment 2	11.45±7.62	5.45±2.91	8.44±6.40	1.67 to 24.62
$POC_{oc\text{-}up}$				
Deployment 1	0.18±0.16	0.46±0.10	0.30±0.20	0.07 to 0.59
Deployment 2	1.34±0.84	0.72±0.68	1.03±0.81	0.00 to 2.65
NEP				
Deployment 1	-1.24±6.83	-2.81±10.22	-1.93±7.95	-13.46 to 6.35
Deployment 2	-8.26±17.93	4.64±20.05	-1.81±19.66	-36.64 to 24.25

Table S3: Average and standard deviation of NEC (mmol C m^{-2} h^{-1}) and $POC_{oc\text{-}up}$ (mmol C m^{-2} h^{-1}) at each site and during each deployment.

	m	b	r	sm	sb	p-value
POCoc_up x NEC	9.39	-1.22	0.87	0.99	1.03	<0.001
$POC_{oc\text{-}up}$ x NEP	-135.83	107.36	-0.16	153.48	124	0.401
NEP x NEC	0.02	6.37	0.04	0.08	1.16	0.819
flow x NEC	1.77	-7.86	0.79	0.26	2.20	<0.001
POCoc_up x flow	0.16	-0.50	0.83	0.02	0.18	<0.001
light x NEC	0	5.23	0.20	0	1.51	0.299
temp x NEC	-31.19	753.76	-0.37	14.57	349.04	0.049
omega x NEC	105.54	-340.71	0.15	133.69	439.55	0.453
omega x NEC for POCoc_up<0.9	6,37	-18.04	0.63	1.78	5.89	0.004
NEP x NEC for POCoc_up<0.9	0.08	2.88	0.58	0.03	0.38	0.009

Table S4: Statistical summary for all relevant Model 2 linear regressions considered. Model 2 regression statistics were calculated using lsqfitma.m, where m is the slope, b is the y-intercept, r is the correlation coefficient, sm is the standard deviation of the slope and sb is the standard deviation of the y-intercept.

Major category (% of transect)	Seg1	Seg2	Seg3	Seg4	Seg5	Seg6	Seg7	Seg8	Seg9
Coral	3	0	0	10	5	0	5	5	1
Macroalgae	10	30	4	0	0	20	5	33	28
Dead coral with algae	7	0	2	0	5	10	0	5	3
Coralline algae	7	0	10	10	10	0	0	3	6
Rubble/Sand	67	40	68	80	70	60	55	47	53

Table S5: Summary of major benthic categories (in %) along nine segments of the reef transect

	Coral Mucus	Zooxanthellae	Fish Feces	Macroalgae
Average $\delta^{13}C$ ($\delta^{13}C$ ranges)	-15.9 (-16.9 – -15)	-14.7 (-15 – -14.5)	-16.5 (-17 – -12)	-17.5 (-18.5 – -15)
% Contribution	30	30	30	10

Table S6: Average $\delta^{13}C$ (‰) associated with each of the components in reef POM, along with associated ranges found in the literature. $\delta^{13}C$ values for coral mucus and zooxanthellae were obtained from a study conducted in Kāne'ohe Bay for the major species in the bay (Rodrigues and Grottoli 2006). Percent (%) contributions of each component were estimated in Wyatt et al. (2013). Weighted average $\delta^{13}C$ of reef POM is -15.7‰.

Deployment 1	***t***	**z**	**TAout**	**TAin**	**DICout**	**DICin**	**F**	ρ
NEC/NCP	±20	±0.15	±2	±2	±2.6	±2.6	±0.12	±0.29
Deployment 2								
NEC/NCP	±20	±0.15	±2	4.85	±2.6	±6.7	±0.18	±0.13
Deployment 1	***t***	**z**	**Mass C**	$\delta^{13}C_{op}$	$\delta^{13}C_{2(3)}$	$\delta^{13}C_{rf}$		
$POC_{oc\text{-}up}$	±20	±0.15	±0.2	±0.2	±0.2	±1.4		
Deployment 2								
$POC_{oc\text{-}up}$	±20	±0.15	±0.2	±1.64	±0.2	±1.4		

Table S7: Uncertainties associated with residence time (*t*, %), depth (z, m), TA (µmol kg^{1}), DIC (µmol kg^{-1}), air-sea CO_2 flux (F, mmol C m^{-2} h^{-1}), density (ρ, kg m^{-3}), mass carbon (%), $\delta^{13}C_{op,}$ $\delta^{13}C_{2(3)}$ and $\delta^{13}C_{rf,}$ which was calculated using the standard deviation between the average (-15.87‰), assuming 100% macroalgae (-17.5‰), and 100% zooxanthellae (-14.7‰).

Dataset S1: Data used to calculate NEC, NEP and $POC_{oc\text{-}up}$

References

Bahr, K. D., Rodgers, K. S., & Jokiel, P. L. (2017). Impact of Three Bleaching Events on the Reef Resiliency of Kāne'ohe Bay, Hawai'i. *Frontiers in Marine Science*, *4*(December). https://doi.org/10.3389/fmars.2017.00398

Chisholm, J. R. M., & Gattuso, J. (1991). Validation of the Alkalinity Anomaly Technique for Investigating Calcification and Photosynthesis in Coral Reef Communities. *Limnology & Oceanography*, *36*(6), 1232–1239.

Courtney, T. A., De Carlo, E. H., Page, H. N., Bahr, K. D., Barro, A., Howins, N., et al. (2018). Recovery of reef-scale calcification following a bleaching event in Kāne'ohe Bay, Hawai'i. *Limnology and Oceanography Letters*, 1–9. https://doi.org/10.1002/lol2.10056

DeCarlo, T. M., Cohen, A. L., Wong, G. T. F., Shiah, F.-K., Lentz, S. J., Davis, K. A., et

al. (2017). Community production modulates coral reef pH and the sensitivity of ecosystem calcification to ocean acidification. *Journal of Geophysical Research: Oceans*, *122*(1), 745–761. https://doi.org/10.1002/2016JC012326

Dickson, A. G., & Millero, F. J. (1987). A comparison of the equilibrium constants for the dissociation of carbonic acid in seawater media. *Deep Sea Research Part A, Oceanographic Research Papers*, *34*(10), 1733–1743. https://doi.org/10.1016/0198-0149(87)90021-5

Dickson, Andrew Gilmore, Sabine, C. L., & Christian, J. R. (2007). *Guide to best practices for ocean CO2 measurements.* North Pacific Marine Science Organization.

Drupp, P., de Carlo, E. H., Mackenzie, F. T., Bienfang, P., & Sabine, C. L. (2011). Nutrient Inputs, Phytoplankton Response, and CO2 Variations in a Semi-Enclosed Subtropical Embayment, Kaneohe Bay, Hawaii. *Aquatic Geochemistry*, *17*(4), 473–498. https://doi.org/10.1007/s10498-010-9115-y

Fagan, K. E., & Mackenzie, F. T. (2007). Air – sea CO2 exchange in a subtropical estuarine-coral reef system , Kaneohe Bay, Oahu, Hawaii, *106*, 174–191. https://doi.org/10.1016/j.marchem.2007.01.016

Ho, D. T., Law, C. S., Smith, M. J., Schlosser, P., Harvey, M., & Hill, P. (2006). Measurements of air-sea gas exchange at high wind speeds in the Southern Ocean: Implications for global parameterizations. *Geophysical Research Letters*, *33*(16), 1–6. https://doi.org/10.1029/2006GL026817

Jokiel, P. (1991). *Illustrated Scientific Guide To Kane'Ohe Bay, Oahu. Hawaii Institute of Marine Biology*. https://doi.org/10.13140/2.1.3051.9360

Jury, C. P., & Toonen, R. J. (2019). Adaptive responses and local stressor mitigation drive coral resilience in warmer, more acidic oceans. *Proceedings of the Royal Society B: Biological Sciences*, *286*(1902), 20190614. https://doi.org/10.1098/rspb.2019.0614

Kohler, K. E., & Gill, S. M. (2006). Coral Point Count with Excel extensions (CPCe): A Visual Basic program for the determination of coral and substrate coverage using random point count methodology. *Computers and Geosciences*, *32*(9), 1259–1269. https://doi.org/10.1016/j.cageo.2005.11.009

de la Moriniere, E. C., Nagelkerken, I., van der Velde, G., Pollux, B. J. a., Hemminga, M. a., & Huiskes, a. H. L. (2003). Ontogenetic dietary changes of coral reef fishes in the mangrove-seagrass-reef continuum: stable isotopes and gut- content analysis. *Marine Ecology Progress Series*, *246*, 279–289. https://doi.org/10.3354/meps246279

Lowe, R. J., Falter, J. L., Monismith, S. G., & Atkinson, M. J. (2009). A numerical study of circulation in a coastal reef-lagoon system. *Journal of Geophysical Research: Oceans*, *114*(6), 1–18. https://doi.org/10.1029/2008JC005081

Mehrbach, C., Culberson, C. H., Hawley, J. E., & Pytkowicx, R. M. (1973). Measurement of the apparent dissociation constants of carbonic acid in seawater at atmospheric pressure. *Limnology and Oceanography*, *18*(6), 897–907. https://doi.org/10.4319/lo.1973.18.6.0897

Page, H. N., Courtney, T. A., De Carlo, E. H., Howins, N. M., Koester, I., & Andersson, A. J. (2019). Spatiotemporal variability in seawater carbon chemistry for a coral reef flat in Kāneʻohe Bay, Hawaiʻi. *Limnology and Oceanography*, *64*(3), 913–934. https://doi.org/10.1002/lno.11084

Pierrot, D., Lewis, E., & Wallace, D. (2006). MS Excel program developed for CO2 system calculations. *ORNL/CDIAC-105a. Carbon Dioxide Information Analysis Center, Oak Ridge National Laboratory, US Department of Energy, Oak Ridge, Tennessee*.

Rodrigues, L. J., & Grottoli, A. G. (2006). Calcification rate and the stable carbon, oxygen, and nitrogen isotopes in the skeleton, host tissue, and zooxanthellae of bleached and recovering Hawaiian corals. *Geochimica et Cosmochimica Acta*, *70*(11), 2781–2789. https://doi.org/10.1016/j.gca.2006.02.014

Shamberger, K., Feely, R., Sabine, C., Atkinson, M., DeCarlo, E., Mackenzie, F., et al. (2011). Calcification and organic production on a Hawaiian coral reef. *Marine Chemistry*, *127*(1–4), 64–75. https://doi.org/10.1016/j.marchem.2011.08.003

Terlouw, G. J., Knor, L. A. C. M., De Carlo, E. H., Drupp, P. S., Mackenzie, F. T., Li, Y. H., et al. (2019). Hawaii Coastal Seawater CO2 Network: A Statistical Evaluation of a Decade of Observations on Tropical Coral Reefs. *Frontiers in Marine Science*, *6*(May), 1–18. https://doi.org/10.3389/fmars.2019.00226

Weiss, R. F. (1974). Carbon dioxide in water and seawater: the solubility of a non-ideal gas. *Marine Chemistry*, *2*, 203–215.

WHP. (1994). *WHP 91-1: World Ocean Circulation Experiment Operations Manual*. Woods Hole, Mass.

Wyatt, A. S. J., Lowe, R. J., Humphries, S., & Waite, A. M. (2013). Particulate nutrient fluxes over a fringing coral reef: Source-sink dynamics inferred from carbon to nitrogen ratios and stable isotopes. *Limnology and Oceanography*, *58*(1), 409–427. https://doi.org/10.4319/lo.2013.58.1.0409